Relative Navigation of Spacecraft Utilizing Bright, Aperiodic Celestial Sources

Suneel I. Sheikh, *ASTER Labs, Inc.*
Paul S. Ray, *U.S. Naval Research Laboratory*
Kathryn Weiner, *Praxis, Inc.*
Michael T. Wolff, *U.S. Naval Research Laboratory*
Kent S. Wood, *U.S. Naval Research Laboratory*

BIOGRAPHY

Suneel Sheikh is Chief Research Scientist at ASTER Labs, Inc. He received his Ph.D. in 2005 from the University of Maryland, where he investigated the use of X-ray pulsars for spacecraft navigation. Prior to this, he has over ten years of industry experience in inertial navigation systems and GPS integration research.

Paul Ray is an Astrophysicist in the Space Science Division of the Naval Research Laboratory. He received his Ph.D. in Physics from Caltech in 1995 for research on radio pulsars. Currently he is active in X-ray timing studies of neutron star and black hole sources, including pulsars and accreting binary systems.

Kathryn Weiner recently graduated from St. John's College in Annapolis, MD, and served as a 2006 summer intern at the Naval Research Laboratory.

Michael Wolff is an Astrophysicist in the Space Science Division of the Naval Research Laboratory. He received his Ph.D. in Astronomy from Indiana University in 1985. He has investigated the properties of a wide range of compact object binary systems, including white dwarf, neutron star, and black hole systems.

Kent Wood is Head of the X-ray/UV Astrophysics and Applications Section at the Naval Research Laboratory. He received his Ph.D. from the Massachusetts Institute of Technology in 1973. He was Principal Investigator of the NRL USA experiment on *ARGOS*, which conducted timing studies and explored applications of X-ray astronomy.

ABSTRACT

Absolute position determination of a single spacecraft can be accomplished utilizing X-ray observations of stable, periodic signals from celestial sources such as pulsars [1]. The utility of this method can be limited by the intrinsic faintness of the signals from the most stable X-ray pulsars, which mandates the use of large area X-ray detectors. However, for many applications, including spacecraft flying in formation for coordinated communication and scientific measurements, only relative range information to another spacecraft is required. Assuming two separate spacecraft carry X-ray detectors, it will be shown that this application does not require the use of stable, periodic X-ray sources. Instead, by cross-correlating the signal received at the two spacecraft from bright X-ray sources that have a large amount of aperiodic variability (e.g. flickering, shot noise, broad band noise, or quasi-periodic oscillations) the distance between the two spacecraft projected in the direction of the X-ray source can be determined directly. Multiple observations of sources in different directions can then be used to fully determine the relative position of the two spacecraft, while requiring only modest size X-ray detectors. Methods to compute this signal cross-correlation are presented. The potential performance of this method is evaluated using realistic simulations of source light curves with Poisson statistics, as well as observations of the most promising X-ray sources made with NASA's *Rossi X-ray Timing Explorer*.

INTRODUCTION

Navigation of spacecraft is a critical component of overall vehicle operations. Most navigation methods are designed to produce position and velocity solutions in an absolute sense, computing these parameters with respect to an inertial reference frame. This allows the vehicle to be guided and controlled with respect to the inertial position of other known objects, including planetary bodies, moons, asteroids, comets, other spacecraft, etc. For some applications, however, determining position and velocity relative to another spacecraft that is in motion is desired. This may include vehicles that must coordinate scientific observations with instruments on each vehicle or perform synchronized communication in coordination with other locations. These vehicles may be following their own free paths, or be following prescribed trajectories such that the multiple vehicles remain in a defined formation, often referred to as *formation flying* [2].

Celestial sources have often been employed as inputs to various spacecraft navigation solution methods. Techniques that incorporate instruments such as star cameras and horizon sensors have typically utilized visible stars whose brightness is essentially constant [3, 4]. Alternative navigation methods have been proposed to make use of variable sources that emit at other wavelengths, such as the radio or X-ray band [1, 5-8]. Much of this navigation research has concentrated on using rotation-powered pulsars, which are rapidly spinning neutron stars that emit periodic signals that are predictable over the long term [9, 10]. This previous work primarily focused on using pulsar's periodic signals to produce accurate full three-dimensional (3-D) inertial position solutions or to aide the computations of integrated numerical position and velocity solutions [8, 11]. This paper will focus on the problem of defining a relative range and range-rate solution between two cooperating space vehicles. In this concept, observational data are shared between vehicles.

Relative navigation can be accomplished by correlating the signal from a variable source as measured by detectors on two or more separate spacecraft. Given sufficient observation time, significantly greater than the light travel time between the two vehicles, the observed pattern of variability at one detector will appear as a delayed version of that seen by the other detector. The measurement of this delay provides a distance measurement between the two detectors, projected along the line of sight to the source, which is assumed to be at effectively infinite distance. There is no requirement that the variability pattern be predictable, which differentiates this from the pulsar-based navigation techniques discussed above. This may prove to be significant since a large number of bright X-ray sources do not exhibit stable pulsations, yet have some level of variability in their emitted radiation. Additionally, when utilizing aperiodic sources in this manner, one does not encounter the integer phase ambiguity problems that can occur with the periodic pulsar-based methods [12].

This paper presents methods of using bright, variable celestial X-ray sources for determining a relative navigation solution between multiple spacecraft. The following section on *Relative Navigation* presents the concepts of this type of spacecraft navigation as well as particular applications for its use. The section on *Aperiodic Sources* presents the types of sources that are useful for this approach, and provides lists of selected candidate sources. The *Analysis Technique* section discusses the specific methods used in the development of this analytical method, as well as the development of simulation tools for evaluating the proposed processes. The *Numerical Comparisons* section provides findings of the analysis using simulated and actual observation data. Finally, some concluding remarks are provided.

RELATIVE NAVIGATION

Various applications such as coordinated communication or scientific observation only require relative distance and speed information, rather than requiring a complete 3-D absolute position and velocity solution for each vehicle. If accurate absolute position and velocity information is known for multiple vehicles, then a relative solution can be directly computed by differencing these solutions between pairs of vehicles. However, absolute solutions may be difficult to obtain in some circumstances, particularly on missions where Global Navigation Satellite System signals are not available, Deep Space Network tracking can not be completed, or solutions may not have the accuracy desired for specific applications [13, 14]. In these cases, a method that directly determines relative position vectors between spacecraft may be beneficial.

It is proposed here to compute relative navigation solutions between pairs of spacecraft at different locations by comparing the measured signal from variable celestial X-ray sources at each spacecraft. Figure 1 presents this concept, where two spacecraft are shown in orbit about Earth while simultaneously measuring the arriving X-radiation from a variable source. This relative navigation concept would be applicable to many multiple vehicle applications, including those in orbit about any planetary body or operating in conjunction on deep space trajectories. By correlating the two signals, a measurement of the position offset of one vehicle with respect to the other can be determined along the direction towards the source. This method requires that both spacecraft are able to observe the celestial source simultaneously, but does not require an unobstructed line of sight between the two vehicles, as long as the data can be communicated between each other at some later time, or through some intermediary method. If there is significant delay between an observation and its data transmission between vehicles, it will be necessary to store vehicle navigation data over this interval to correctly compute a relative navigation solution.

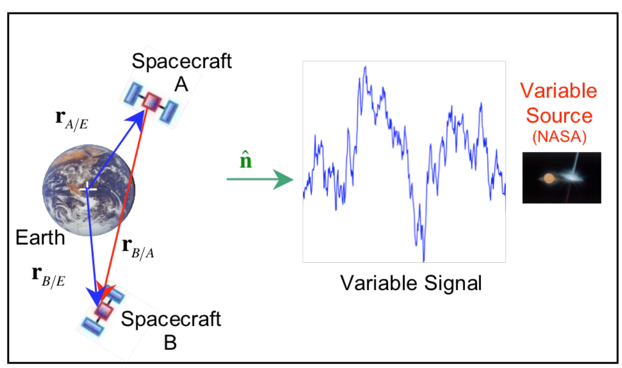

Figure 1. Relative navigation between two spacecraft observing the same variable celestial source.

The X-radiation emitted from these sources is measured at each spacecraft via the detection of individual X-ray photons. The photons detected by each spacecraft are distinct and independent, thus a measurement is not made through direct comparison of individual photon arrival times. Rather, a comparison of the time variability of the *rate* of detection of X-ray photons at each detector is computed. Because these rates are determined by photon counting, they are described by Poisson statistics, thus there will be a large amount of variability in the observed light curve simply due to counting statistics. This portion of the signal variability is *uncorrelated* between the two detectors, and only the *correlated* portion of each signal contains useful information content for a relative range measurement.

The diagram in Figure 2 shows the basic geometry of the relative range between two spacecraft with respect to the variable source. The relationship of measured offset between the two signals is shown in two dimensions. To first order, by assuming the difference in the relativistic effects is negligible, the range difference, $\Delta\rho$, along the direction to the source, $\hat{\mathbf{n}}$, is related to the measured time difference, Δt, and *c*, the speed of light, by

$$\Delta\rho = \hat{\mathbf{n}} \cdot \left(\mathbf{r}_B - \mathbf{r}_A\right) = \hat{\mathbf{n}} \cdot \Delta\mathbf{x} = c\Delta t \qquad (1)$$

In Eq. (1), $\Delta\mathbf{x}$ is the relative position vector between the two spacecraft. Although relativistic effects are present in principle [15, 16], for the purposes of this paper, these effects will be considered negligible.

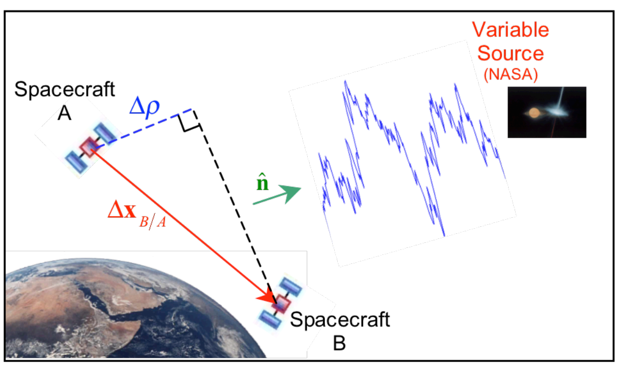

Figure 2. Distance offset of spacecraft along line of sight to source.

The accuracy of this navigation method is determined by the precision of the determination of Δt. From Eq. (1), determining relative timing accuracies to within 1 ms produces range accuracies on the order of 300 km, whereas accuracies on the order of 1 μs yield 0.3 km range accuracies. The desired accuracy would depend on a specific application. With multiple sequential measurements, evaluating the rate of change of range provides an estimate of relative range-rate in the direction of the source. Also with multiple measurements, particularly from multiple sources, an estimate of a full 3-D relative navigation solution can be created.

Since this type of relative navigation shares information between two spacecraft, the measured data must be transmitted between vehicles, or alternatively both data sets must be transmitted to the ground for post-processing. Once the observed data from each vehicle are in one central processing location the correlation may be computed. The relative navigation scheme could be implemented in a variety of methods. For example, one spacecraft may have a large area detector array used for measuring the X-ray photon arrival, and all remaining spacecraft could have smaller sized detectors. This concept of a single *base-station* spacecraft and other *remote* spacecraft (or *parent-child* concept) may have all measured data transmitted to the base station. After processing onboard the base-station, the relative navigation information between the main base-station and each remote vehicle would be transmitted to those vehicle that require this information. An alternative technique would be to utilize identical detectors on all spacecraft and maintain data communication between all vehicles such that each spacecraft can compute a relative navigation solution to other vehicles as needed. This *symmetric* scheme is useful when all spacecraft require constant communication between one another, and does not identify a hierarchy between vehicles. Depending on the type of communication, especially one that can encode time information with the data transmission for a preliminary range estimate, the methods discussed here can supplement this estimate as needed. The accuracies of particular solutions may vary depending upon a specific vehicle scenario. Investigations should be pursued to optimize the system design for a specific use case.

APERIODIC SOURCES

The class of celestial sources that is useful for this relative navigation technique includes bright X-ray sources with large amounts of rapid variability. Nearly all of the bright X-ray point sources in the sky are X-ray binaries containing a compact object (neutron star or black hole) accreting material from a stellar companion. Through the gravitational fields of the binary system, the flow of material typically coalesces onto an accretion disk about the compact companion, as shown in Figure 3. The accretion process is highly unstable and many of these sources exhibit pronounced variability over a broad range frequency scales up to about 1000 Hz. This variability can take the form of red noise, broadband noise, shot noise, periodicities, and quasi-periodic oscillations (QPOs). Any source with strong variability, including pulsars, can in principle be useful. The analysis presented here works equally well for periodic or aperiodic sources (although the periodic sources can suffer from integer phase ambiguity issues). Since the methods do not exploit the periodic nature of the sources, nor require any kind of model for the pulse arrival times of the source, the generalized term *aperiodic sources* is used in the text.

In addition to the short timescale variability, many of these sources exhibit transient behavior, when a source that normally is extremely faint brightens by a factor of 1000 or more [17]. The transient outbursts in these sources can last from hours to years, with most outbursts lasting one to several months. The recurrence times of these outbursts vary from a year to decades, or longer. The flux from sources with predominantly persistent radiation, is also highly variable, being modulated by changing mass transfer rates, viscous processes in the accretion disk, oscillations, instabilities in the accretion disk, etc. [17]. The fastest observable timescales are expected to be the gravitational dynamical timescale at the inner edge of the accretion disk, which is roughly 1500 Hz for neutron stars and 150 Hz for stellar-mass black holes [18].

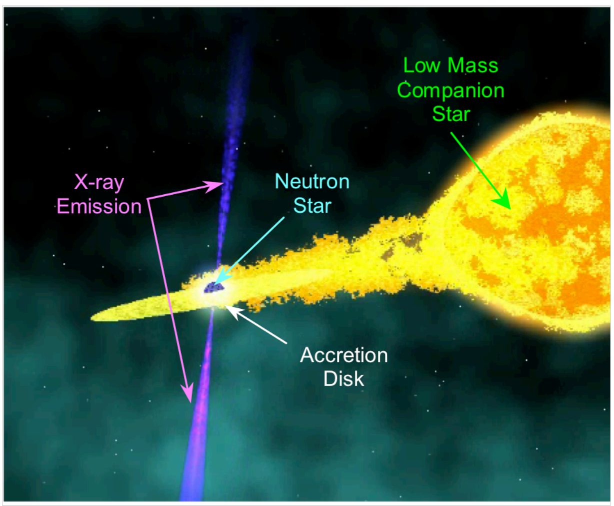

Figure 3. Low-mass X-ray binary star system.

The measured power spectrum of the source can be used to characterize the type of variability produced. Some examples of observed power spectra for different source classes are shown in Figure 4 – Figure 6. The data used to compute these spectra were obtained from NASA's *Rossi X-ray Timing Explorer* (*RXTE*) [19]. In Figure 4, the Crab pulsar (PSR B0531+21) shows strong signal power only at 30 Hz and several harmonics, due to its periodic signal, whereas the pulsar in Hercules X-1 (B1656+354) shows some broad-band noise in addition to the 0.8 Hz pulsations [20]. In Figure 5, the spectrum of the black hole candidate high-mass X-ray binary Cygnus X-1 (B1956+350) shows strong red noise [21], whereas the spectrum from the transient black hole binary GRS 1915+105 (Nova Aquila 1992) shows band-limited noise plus several strong QPOs [22]. Sources such as these have highly variable signals across a broad range of frequencies. The spectrum of the atoll source 4U 1728-34 is shown in Figure 6, with a strong, narrow QPO visible at approximately 900 Hz [23]. In contrast, the spectrum of the exotic X-ray binary system Circinus X-1 (B1516-569) shows only weak variability at all frequencies during this particular observation [24].

A useful catalogue of bright X-ray sources is based on over a decade of continuous monitoring of the X-ray sky with the All-Sky Monitor (ASM) instrument aboard *RXTE* [25]. The ASM was designed to monitor the X-ray sky in the 1.5–12 keV energy band using three steerable coded-aperture cameras [26]. This survey type instrument provides continuous sky coverage of bright X-ray sources. Sources that are still potentially relevant to the relative navigation technique, but may not be in the ASM catalogue, include transients that haven't been active during the *RXTE* mission (1995–present).

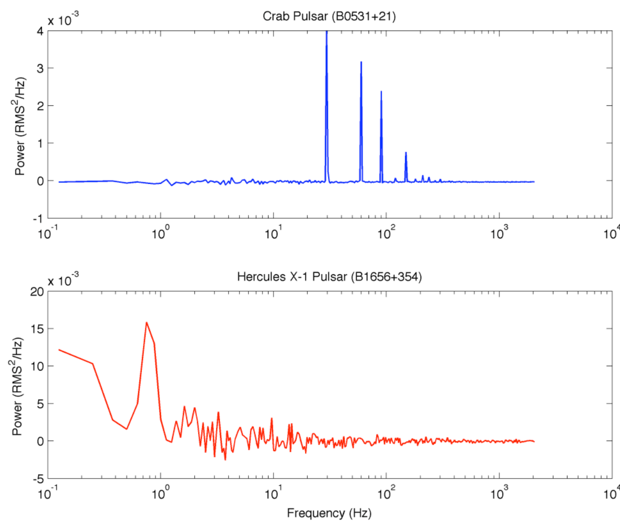

Figure 4. Power spectra of the rotation-powered Crab pulsar and the accreting pulsar Hercules X-1.

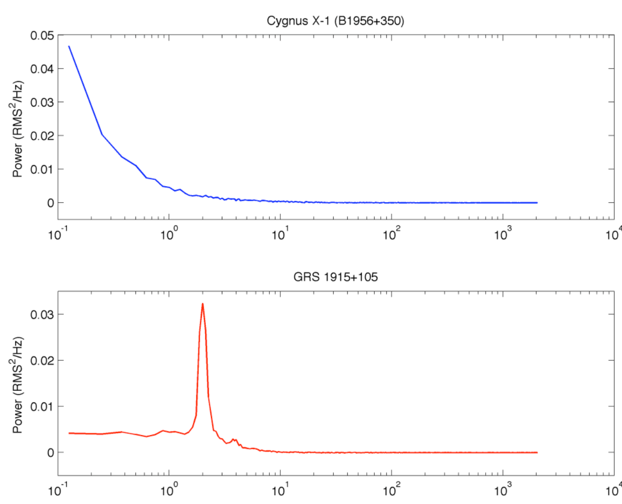

Figure 5. Power spectra of two black hole systems. Cygnus X-1 shows pure red noise, while GRS 1915+105 has band-limited noise plus strong QPOs.

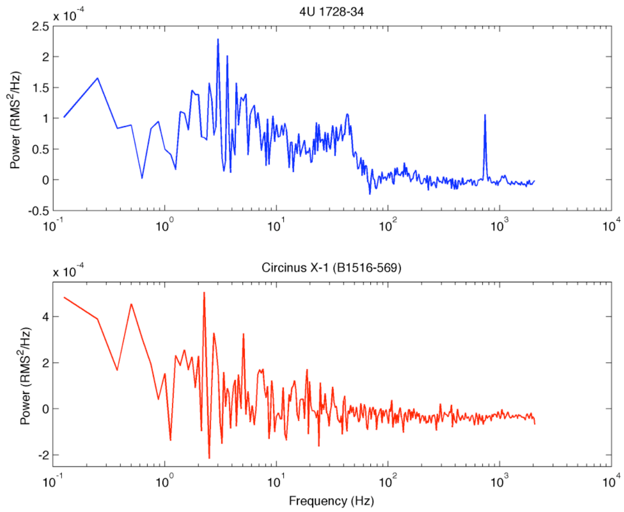

Figure 6. Power spectra of the neutron star 4U 1728-34 showing a kHz QPO, and Circinus X-1 with weak variability.

The accuracy of an offset measurement with a particular source will depend on the total photon count rate from the source, the total fractional variability, and the frequency distribution of the variability power. However, it is a challenge to define a precise figure of merit based on these quantities primarily because there is no single number to characterize the frequency distribution of the power. In addition, accreting sources are frequently transient and also make rapid transitions from one spectral state to another [17]. During the state transitions, there may be striking differences in each of the count rate, variability, and frequency distribution quantities. Selecting a source as a good navigation candidate at any given time will be a challenge without a short observation to determine its current state.

ANALYSIS TECHNIQUE

The fundamental measurement required for the relative navigation technique is the precise determination of the offset between two noisy realizations of a variable rate time series. The analysis tool employed for this task is the *cross-correlation* between the two measured time series. A discussion of this analysis method is provided below, as well as a simulation created to estimate its performance.

To illustrate the analysis method step by step, a time series was generated that contains strong, aperiodic variability. This represents the time variable brightness of an X-ray source. A second, identical, copy of this series is then shifted by a known amount. These time series are shown in Figure 7 where the shift is chosen to be ten samples. These represent a signal that would be observed by two X-ray detectors, D1 and D2, in the absence of Poisson noise, separated by a distance equal to $c10\Delta t_{sample}$ in the direction towards the source. In this figure D2 is *farther* from the source than D1, so the signal in D2 *lags* that seen in D1. The model uses an average photon count rate of eight counts per bin, and other than the fixed offset, the series are identical.

Real X-ray detectors onboard spacecraft, however, will not directly measure the instantaneous brightness of a source. Rather, they must estimate the brightness of a source by counting individual X-ray photons detected over a short interval of time, which means that the actual measured count rates obey Poisson, or *counting*, statistics. Using the flux time series as the rate of a Poisson process, which is independent for detectors D1 and D2, results in the simulated time series as shown in Figure 8. This models what these two independent X-ray detectors would individually count from an X-ray source with this count rate. The fact that these are both measurements of identical brightness variations is somewhat obscured by the Poisson fluctuations inherent in the detection process. The Poisson fluctuations have the effect of adding *white noise* (noise of equal strength at all frequencies) to the measurement. The *standard deviation* of this noise in a particular time series bin is equal to the square root of the number of counts in that bin, so this noise is most important when the number of counts in each bin is small, as is nearly always the case for X-ray sources sampled at high time resolution.

To measure the offset between two time series, the cross-correlation of the two series is computed. The cross-correlation function between two discretely sampled time series, g and h, is defined as,

$$\mathrm{corr}(g,h)_j \equiv \sum_{k=0}^{N-1} g_{j+k} h_k \qquad (2)$$

In Eq. (2), the correlation is computed over a set of lags, j in the range $-M$ to M, where M is the maximum lag of interest [27]. The correlation will be maximized when j is the negative of the offset between the two time series. The correct offset is then measured by finding the peak in the cross-correlation function after searching over an appropriate range of lags. This immediately provides the result with an uncertainty of one time series bin. Fitting a model function, such as a Gaussian or Lorentzian, to the cross-correlation profile helps determine this offset to sub-bin accuracies.

Figure 9 shows the cross-correlation amplitude of Eq. (2), normalized by the sum of squares of one time series so that 1.0 represents a perfect correlation, using the two time series of Figure 8. The strong correlation peak at a lag (offset) of ten bins between these two time series is clearly visible. The peak is located at a positive lag, indicating that the series D2 lags (as opposed to leads) series D1.

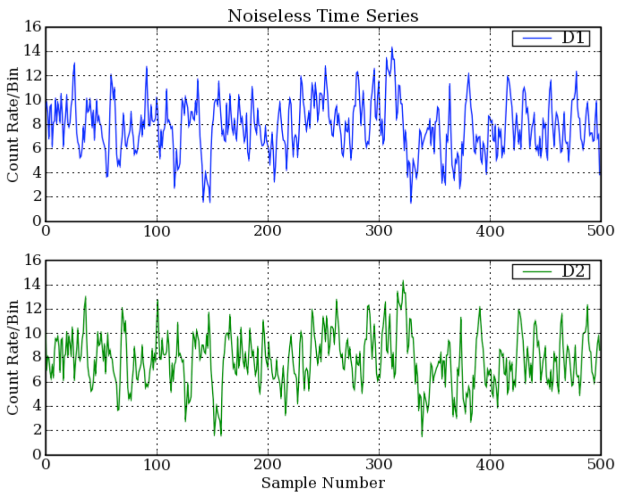

Figure 7. Two identical noiseless time series, with series D2 delayed with respect to D1 by 10 bins.

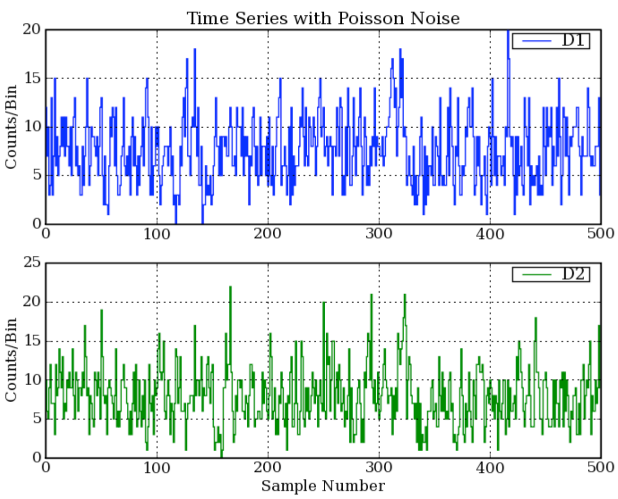

Figure 8. The two time series from Figure 7 with added Poisson noise. Within the series, each bin is an independent Poisson random variate with the rate corresponding to the value of the noiseless time series.

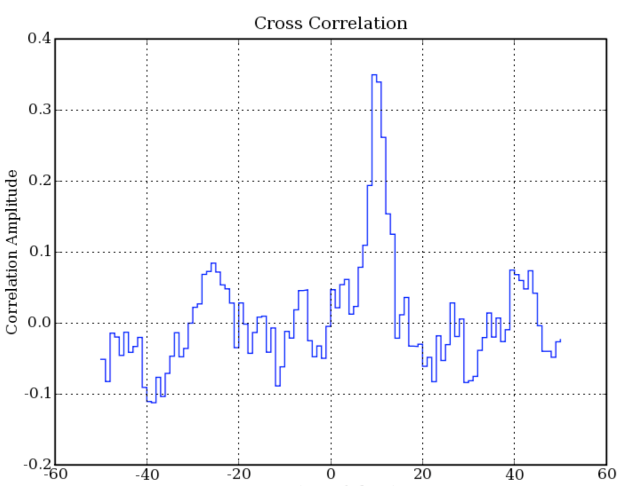

Figure 9. The cross correlation amplitude as a function of lag between the two time series in Figure 8.

NUMERICAL COMPARISONS

The time series cross-correlation technique presented in the previous section provides a method to measure the range based upon cross-correlating X-ray photon time series. In this section the actual performance of the technique is investigated by performing the analysis on both simulated data sets and actual data obtained from *RXTE*. The simulations provide a way to evaluate the scaling of the accuracy with various parameters of the source and detector, while actual data provide a valuable verification of the simulations and a demonstration of the technique in real world conditions.

Simulated Data Sets

In order to evaluate the potential of the relative navigation methods using celestial X-ray sources, a simulation of the variable signals from these sources was developed. These simulations allowed the characterization of the accuracy of the method as a function of various parameters including the detected photon count rate, the observation duration, and highest frequency variability present in the signal.

For all of the simulations, the time series variability was modeled with a zero-centered Lorentzian power spectrum, $P(\nu)$, as a function of frequency, ν, of the form [28],

$$P(\nu) = \frac{R^2 \Delta}{\pi\left(\Delta^2 + \left(\nu - \nu_0\right)^2\right)} \tag{3}$$

In Eq. (3), Δ is the half width half maximum (HWHM) of the Lorentzian model (and is not "delta" as in the previous equations). Since the Lorentzian was chosen as zero-centered, or $\nu_0 = 0$, the characteristic frequency of the power spectrum is $\nu_{max} = \Delta$. When $\nu_0 = 0$, the fractional RMS integrated over positive frequencies is $R/2$, while for $\nu_0 >> \Delta$ the fractional RMS approaches R. The power spectrum was converted to a time series by assigning uniform random phases to each frequency and performing an inverse Fourier Transform. Two independent Poisson realizations of this time series were then created to simulate two detectors observing the signal. These time series were then cross-correlated and the peak of the correlation was determined by fitting a Lorentzian function to the correlation amplitudes. The centroid of this fit is the measured offset. This process was repeated 50 times and the standard deviation of the measured offsets determined the measurement error assigned to that simulation.

The simulation results for correlation timing accuracy versus the source characteristic frequency are provided in Figure 10. The plot was created using 50 s observation duration and a bin size of 0.1 ms. The average source count rate was set to 2500 ph/s. The variability from the simulated source was modeled as a zero-centered

Lorentzian function with fractional RMS equal to 0.15 (R = 0.3). The characteristic frequency was varied over the range 3 to 316 Hz. A best-fit model is also shown through the simulated data points. The model shows the accuracy improves as $\Delta^{-2/3}$.

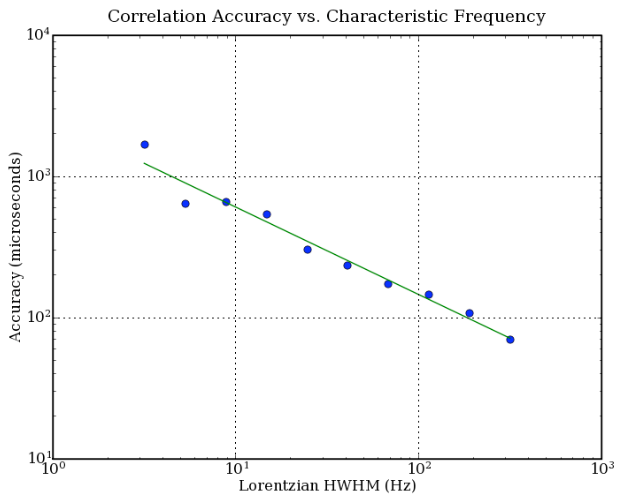

Figure 10. Cross-correlation accuracy as a function of source variability frequency (Δ), modeled as a zero-centered Lorentzian function with fractional RMS equal to 0.15.

Figure 11 provides the simulated timing accuracy versus the detected photon count rate, H, of a source. The count rate depends on the product of the source X-ray flux, F_S, and the detector area, A, such that $H = F_S A$. In this analysis, the background rate in the detector from unvetoed charged particles and the diffuse X-ray background is ignored. For bright sources, this background is typically negligible and only slightly decreases the observed RMS of the source. The plot was created by modeling a zero-centered Lorentzian function, with characteristic frequency of 200 Hz and a fractional RMS of 0.15. The observation time is selected as 50 s and a bin size of 1 ms. The best-fit model yields an accuracy proportional to $H^{-0.96}$, indicating that the accuracy improves essentially linearly with total count rate.

Figure 12 provides the expected accuracy as a function of observation time. This plot was created using a count rate of 500 ph/s, fractional RMS of 0.15, and characteristic frequency of 100 Hz. The bin size was selected to be 1 ms. A best-fit model to this data shows that accuracy decreases as observation time increases, with a slope of $t_{obs}^{-0.57}$, which closely matches an expected inverse square-root dependency on observation time. The simulation results can be summarized in the following relationship,

$$\sigma \propto (F_S A)^{-1} t_{\text{obs}}^{-1/2} \Delta^{-2/3} \quad (4)$$

Eq. (4) describes the scaling of the accuracy with several source and instrumental parameters. Additional analysis is required to completely define this relationship.

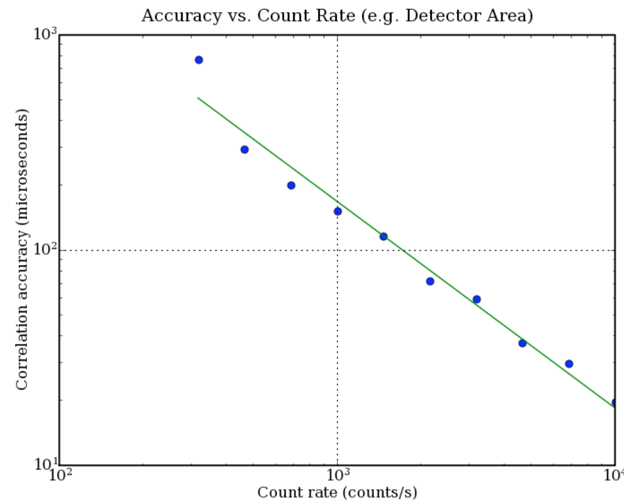

Figure 11. Series cross-correlation accuracy as a function of source photon count rate.

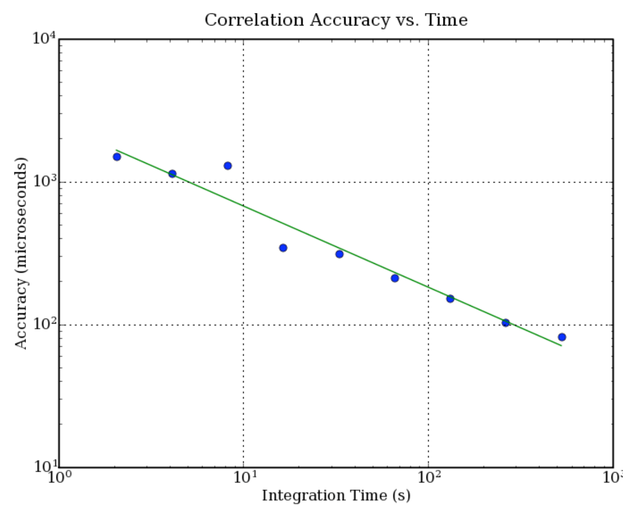

Figure 12. Series cross-correlation accuracy as a function of integrated observation time.

Real X-ray Data Sets

Although simultaneous observations of appropriate bright X-ray sources with two different satellites are not currently available, a demonstration of this technique can be performed using the Proportional Counter Array (PCA) aboard *RXTE*. The PCA consists of five essentially identical and independent proportional counter units (PCUs), which provides a large area detector (~1250 cm^2/PCU) with high time resolution (~1 μs) in the 2–60 keV energy band [29]. This allows experiments where the time series from one PCU is correlated against that taken by an adjacent PCU. Since the PCUs are arranged in a plane perpendicular to the direction towards the source, there is no significant time delay to be measured that would represent position offset. However, an analysis of the error in measuring the zero offset between PCUs is still useful, since, to first order, this does not change as a function of the distance between the two detectors.

To perform this demonstration, it is necessary to identify appropriate data sets from candidate sources. The large-area PCA can record tens of thousands of X-ray counts per second when pointed at bright sources. Because of telemetry limitations, all information on each recorded count is not normally telemetered to the ground. Rather, the data streams from each PCU are passed to the onboard Experiment Data System (EDS) computer, which has many programmed data modes that can reduce the telemetry rate. The choice of modes for a particular observation is made by the principal investigator for that observation to balance the science objectives with the telemetry rate limitations. Since only publicly available archival observations are used in this investigation, it was necessary to search for observations with appropriate data modes. The most important parameter is that the mode *must* preserve the identity of the PCU for each recorded photon. This eliminated all binned and single bit data modes, and many of the event data modes from consideration. The analysis was also restricted to data sets with 125 μs or better time resolution, and which did not include a cutoff for only high energies that reduced the useful count rate to a small fraction of the total source rate.

An analysis of the ASM catalogue shows at least 40 sources with flux greater than a selected cutoff value of approximately one-tenth of the Crab pulsar flux. The preliminary analysis of this research chose to investigate the top 20 sources in this list. In addition to the strictly aperiodic sources, a few pulsars, including the Crab (PSR B0531+21), Centaurus X-3 (B1119-603), and Hercules X-1 (B1656+354) are included in the list. Observations from all candidate sources were selected based upon the data mode requirements described above. Power spectrum plots were generated to determine the total fractional RMS variability and the frequency distribution of the variability for each observation. Observations of sources with little variability were discarded for this analysis. Photon arrival times from a good observation were then binned appropriately (either 1/4096 or 1/2048 second bin times depending on the event data mode) for each PCU. Then a cross-correlation of two PCU data sets was performed using a range of interval lengths from 25 to 2000 seconds. Figure 13 shows two cross-correlation curves for sample observations of Cygnus X-1 and GRS 1915+105. These plots include the best-fit model Lorentzian function that was used to measure the centroid of the peak. The cross correlation accuracies are then determined as the standard deviation of the measurements made over many intervals of a particular length.

To demonstrate results from these analysis techniques several representative data sets are provided using the *RXTE* science observation archives. For the Crab pulsar (B0531+21), an observation on 17 July 2000 was chosen, with duration of about 1980 s and an average count rate of 3350 ph/s/PCU. For GRS 1915+105, a 1320 s observation on 7 May 2004 with 1700 ph/s/PCU, and for Cygnus X-1 (B1956+350), a 1380 s observation on 6 August 1996 with 1200 ph/s/PCU were selected. The averaged correlation error using the methods described above is plotted for these three sources in Figure 14 as a function of integration time. Power-law fits to the data are also provided, which closely obey the simulated $t_{obs}^{-1/2}$ scaling. The best accuracies are attained using the very bright and highly modulated Crab pulsar, with the two aperiodic sources coming in about an order of magnitude poorer. However, it is important to note that these accuracies are attained without *any* prior information about the source, including any ephemeris data. Other than requiring the two separate detectors to be pointed at the same source, which only requires direction knowledge of individual sources, no information about their specific variability needs to utilized within the cross-correlation techniques. This is significant when compared to other proposed methods of spacecraft navigation, which do require current, accurate source ephemeris and timing models [1].

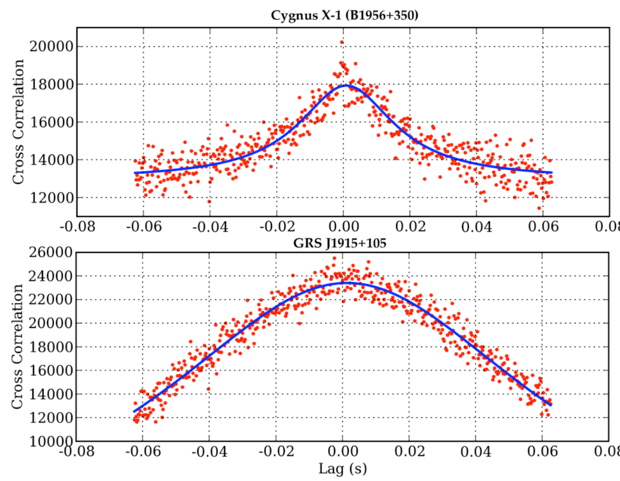

Figure 13. Example real data correlation plots.

For future relative navigation systems, several detector system improvements could be considered to enhance the performance. These would include increased detector area, improved quantum efficiency, lower background rates, and longer observation durations. In addition several processing enhancements could be used such as optimizing the energy band selected to maximize the accuracy, and potentially prefiltering the data before cross correlation to reduce the white noise at frequencies that are not useful. Further studies are planned to investigate improvements to the analysis techniques, including alternative model functions for the fitting process other than Lorentzian functions, switching to the frequency domain for the cross-correlation process using method such as that described by Taylor [30]. In addition applications with two dissimilar detector areas will be considered, and classification of bright, aperiodic sources to assess their utility for these purposes will be undertaken.

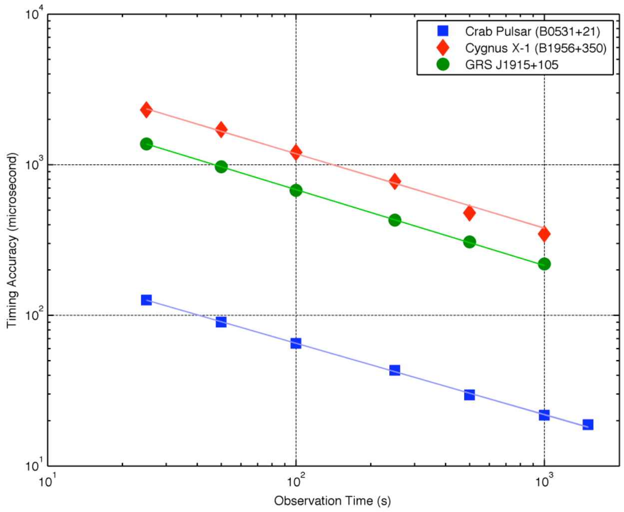

Figure 14. Average correlation error from three source observations obtained with *RXTE*.

CONCLUSIONS

Methods to determine the relative range between two spacecraft are important for several applications. Using the signal from variable X-ray sources could potentially provide high accuracy range measurements between vehicles. This paper has presented a preliminary analysis of the technique, including Monte Carlo simulations that demonstrate the scaling of the accuracy with various parameters. This technique has also been demonstrated using real data from *RXTE*, with preliminary results providing sub-millisecond accuracy. Future planned research anticipates that these accuracies will improve using refined techniques and additional sources.

ACKNOWLEDGMENTS

Basic research in X-ray Astronomy at NRL is supported by NRL/ONR. This research has made use of data obtained from the High Energy Astrophysics Science Archive Research Center (HEASARC), provided by NASA's Goddard Space Flight Center. We also gratefully acknowledge the catalog and light curves provided by the ASM/*RXTE* team.

REFERENCES

[1] Sheikh, S. I., Pines, D. J., Wood, K. S., Ray, P. S., Lovellette, M. N., and Wolff, M. T., "Spacecraft Navigation Using X-ray Pulsars," *Journal of Guidance, Control, and Dynamics*, Vol. 29, No. 1, 2006.

[2] Bauer, F. H., Hartman, K., How, J. P., Bristow, J., Weidow, D., and Busse, F., "Enabling Spacecraft Formation Flying through Spaceborne GPS and Enhanced Automation Technologies," *ION-GPS Conference*, Nashville, TN, September 1999.

[3] Gounley, R., White, R., and Gai, E., "Autonomous Satellite Navigation by Stellar Refraction," *Journal of Guidance, Control, and Dynamics*, Vol. 7, No. 2, 1984, pp. 129-134.

[4] Battin, R. H., *An Introduction to the Mathematics and Methods of Astrodynamics*, Revised ed., American Institute of Aeronautics and Astronautics, Washington, DC, 1999.

[5] Downs, G. S., "Interplanetary Navigation Using Pulsating Radio Sources," *NASA Technical Reports N74-34150*, 1974, pp. 1-12.

[6] Chester, T. J., and Butman, S. A., "Navigation Using X-ray Pulsars," *NASA Technical Reports N81-27129*, 1981, pp. 22-25.

[7] Wood, K. S., "Navigation Studies Utilizing The NRL-801 Experiment and the ARGOS Satellite," *Small Satellite Technology and Applications III*, Ed. B. J. Horais, International Society of Optical Engineering (SPIE) Proceedings, Vol. 1940, 1993, pp. 105-116.

[8] Sheikh, S. I., "The Use of Variable Celestial X-ray Sources for Spacecraft Navigation," Ph.D. Dissertation, University of Maryland, 2005, URL: https://drum.umd.edu/dspace/handle/1903/2856.

[9] Manchester, R. N., and Taylor, J. H., *Pulsars*, W.H. Freeman and Company, San Francisco CA, 1977.

[10] Lyne, A. G., and Graham-Smith, F., *Pulsar Astronomy*, Cambridge University Press, Cambridge UK, 1998.

[11] Sheikh, S. I., and Pines, D. J., "Recursive Estimation of Spacecraft Position Using X-ray Pulsar Time of Arrival Measurements," *ION 61st Annual Meeting*, Institute of Navigation, Boston MA, 27-29 June 2005.

[12] Sheikh, S. I., Golshan, A. R., and Pines, D. J., "Absolute and Relative Position Determination Using Variable Celestial X-ray Sources," *30th Annual AAS Guidance and Control Conference*, American Astronautical Society, Breckenridge, CO, 3-7 February 2007.

[13] Parkinson, B. W., and Spilker, J. J. J. Eds., *Global Positioning System: Theory and Applications, Volume I*. American Institute of Aeronautics and Astronautics, Washington, DC, 1996.

[14] Thornton, C. L., and Border, J. S., *Radiometric Tracking Techniques for Deep Space Navigation*, John Wiley & Sons, Hoboken, NJ, 2003.

[15] Hellings, R. W., "Relativistic Effects in Astronomical Timing Measurements," *Astronomical Journal*, Vol. 91, 1986, pp. 650-659.

[16] Backer, D. C., and Hellings, R. W., "Pulsar Timing and General Relativity," *Annual Review of Astronomy and Astrophysics*, Vol. 24, 1986, pp. 537-575.

[17] van der Klis, M., "Rapid X-ray Variability," *Compact Stellar X-ray Sources*, W. Lewin and M. van der Klis Eds., Cambridge University Press, Cambridge, UK, 2006, pp. 39-112.

[18] King, A., "Accretion in Close Binaries," *X-ray Binaries*, W. H. G. Lewin, J. van Paradijs, and E. P. J. van den Heuvel Eds., Cambridge University Press, Cambridge UK, 1995, pp. 419-456.

[19] Bradt, H. V., Rothschild, R. E., and Swank, J. H., "X-ray Timing Explorer Mission," *Astronomy and Astrophysics Supplement Series*, Vol. 97, 1993, pp. 355-360.

[20] Still, M., O'Brien, K., Horne, K., Hudson, D., Boroson, B., Vrtilek, S. D., Quaintrell, H., and Fiedler, H., "RXTE Observations Of Hercules X-1 During The 1998 July Short High State," *The Astrophysical Journal*, Vol. 553, 2001, pp. 776-787.

[21] Belloni, T., and Hasinger, G., "An Atlas of Aperiodic Variability in HMXB," *Astronomy and Astrophysics*, Vol. 230, 1990, pp. 103-119.

[22] Markwardt, C. B., Swank, J. H., and Taam, R. E., "Variable-Frequency Quasi-Periodic Oscillations From The Galactic Microquasar GRS 1915+105," *The Astrophysical Journal*, Vol. 513, 1999, pp. L37-L40.

[23] Strohmayer, T. E., Zhang, W., Swank, J. H., Smale, A., Titarchuk, L., Day, C., and Lee, U., "Millisecond X-ray Variability From An Accreting Neutron Star System," *The Astrophysical Journal*, Vol. 469, 1996, pp. L9-L12.

[24] Saz Parkinson, P. M., Tournear, D. M., Bloom, E. D., Focke, W. B., Reilly, K. T., Wood, K. S., Ray, P. S., Wolff, M. T., and Scargle, J. D., "Long-Term X-ray Variability of Circinus X-1," *The Astrophysical Journal*, Vol. 595, 2003.

[25] RXTE Science Operations Facility, "XTE ASM Catalog," [online], URL: http://rxte.gsfc.nasa.gov/docs/xte/SOF/ASM_Catalog.html [cited 15 October 2006].

[26] Levine, A. M., Bradt, H., Cui, W., Jernigan, J. G., Morgan, E. H., Remillard, R., Shirey, R. E., and Smith, D. A., "First Results From The All-Sky Monitor On The Rossi X-ray Timing Explorer," *The Astrophysical Journal*, Vol. 469, 1996, pp. L33-L36.

[27] Chattfield, C., *The Analysis of Time Series*, Sixth ed., Chapman & Hall/CRC, Boca Raton, FL, 2004.

[28] Belloni, T., Psaltis, D., and van der Klis, M., "A Unified Description Of The Timing Features Of Accreting X-ray Binaries," *The Astrophysical Journal*, Vol. 572, 2002, pp. 392-406.

[29] Jahoda, K., Swank, J. H., Giles, A. B., Stark, M. J., Strohmayer, T., and Zhang, W., "In Orbit Performance and Calibration of the Rossi X-ray Timing Explorer (RXTE) Proportional Counter Array (PCA)," *Proceedings of SPIE -- Volume 2808*, The International Society for Optical Engineering, 9 July 1996.

[30] Taylor, J. H., "Pulsar Timing and Relativistic Gravity," *Philosophical Transactions of the Royal Society of London*, Vol. 341, 1992, pp. 117-134.